Hindawi
Advances in Civil Engineering
Volume 2021, Article ID 6672301, 12 pages
https://doi.org/10.1155/2021/6672301

Research Article

Research on the Collapse Coefficient of Collapsible Loess under Unloading

Bin Zhi,[1] **Pingping Wei**,[1] **Xiaochan Wang**,[1] **Zengyue Li**,[1] **Yilong Ren**,[2] **Hui Zhang**,[1] **Jinhua Li**,[1] **and Botuan Deng**[1]

[1]*School of Architecture and Civil Engineering, Xi'an University of Science and Technology, Xi'an 710054, China*
[2]*The Logistics Support Department of the PLA Military Commission of the People's Liberation Army Resettlement Housing Support Center, Beijing 100089, China*

Correspondence should be addressed to Bin Zhi; xianzhibin@163.com

Received 19 November 2020; Revised 11 January 2021; Accepted 20 January 2021; Published 13 February 2021

Academic Editor: Jian Xu

In the geogenetic overburden excavation of underground space projects (such as comprehensive pipe corridors or subways), the foundation stress is in an unloading state. The effect(s) from the unloading on the coefficient of subsidence in the loess area should be considered. In this study, to explore the effect of unloading on the collapsibility of loess, the collapsible loess in the Guanzhong area was considered as the research object. An expression for the unloading collapse coefficient was established based on the unloading stress ratio, unloading collapse ratio, and other parameters. The influence of the unloading on the loess collapse coefficient was studied using an indoor collapsibility test, and the function form and parameters for the expression were determined. As combined with the field test, the accuracy of the expression for the unloading coefficient was verified based on the test value for the specific collapsibility, calculated value for the specific collapsibility, and calculated value for the unloading collapsibility.

1. Introduction

The contradiction between the rapid expansion of China's urban space demands and limited space resources has become increasingly prominent. As the main carrier of urban infrastructure, underground space has been developed on a large scale, and, accordingly, new underground space projects (such as comprehensive pipe galleries and subways) are continuously being planned and constructed. However, owing to the excavation of the upper soil, the foundation stress is less than the self-weight stress of the original overburden soil; thus, the foundation stress is in an unloading state. In the loess region, if the collapsibility evaluation and subsequent foundation treatment design are conducted according to the "Building Code for Collapsible Loess Region" (GB-50025-2018) [1], the safety coefficient will be excessively high, causing unnecessary economic losses and conflicting with the economic principles. Therefore, based on previous studies, this study analyzes and studies loess collapsibility under unloading.

For nearly a half-century, experts and scholars from various countries have conducted qualitative and quantitative research on collapsible loess. In 1966, China issued the first special code for the loess area, that is, "Building Code for Collapsible Loess Area" (BJG-20-66), and gradually introduced the "78 Code," "90 Code," and "04 Code"; the latest "18 Regulations" code provides guarantees of construction safety in the loess area.

Liu et al. [2, 3] recognized the special structure of loess earlier and pointed out that the collapsibility of loess is extremely harmful to engineering construction in loess area. Chen and Liu [4] obtained several laws of collapsible deformation of loess through laboratory tests and suggested that the collapsible loess should be treated in different regions. Shao et al. [5] believed that the initial pressure has an important influence on the deformation of collapsible loess.

Through the study of loess particles, Assallay [6, 7] realized that a certain amount of clay minerals was necessary for collapsibility, but, with an increase in clay content, the loess state would change from collapsibility to non-collapsibility. Shen et al. [8, 9] regarded natural loess as a heterogeneous material composed of cemented blocks and weak belts and, based on this analysis, established a binary medium model for loess.

Zhu et al. [10] analyzed the influences of eight soil property indexes (including the pore ratio, dry density, and initial moisture content) on the collapse coefficient and established a regression equation for the loess collapse coefficient and each influencing factor. Liu [11] conducted a detailed analysis of a collapse coefficient of loess and its influencing factors in several areas in northwest China and established a regression relationship between the collapse coefficient and influencing factors.

Wang and Liu [12] derived a collapse coefficient correction formula by setting a correction scale factor and used this factor to correct a collapse coefficient calculated in a laboratory experiment. Hu et al. [13, 14] reported that the collapse coefficient of loess increases more significantly at low pressures under special circumstances and showed that the stability time for loess collapsibility was prolonged under various pressures. Chen et al. [15–17] believed that the discontinuous distribution of the collapsible loess and complex engineering geological conditions in large thick loess resulted in a high level of collapsibility. Gao et al. [18] established a calculation method for a principal component score for the collapse coefficient by analyzing changes in the structural parameters before and after the collapse.

At present, most research studies on soil collapsibility are conducted under constant pressure and without considering the influence of the upper stress changes on it. However, in practical engineering, the influence of the unloading on the strength characteristics of the geotechnical materials cannot be ignored.

Using laboratory tests, Yang et al. [19, 20] found that the unloading rate had a significant impact on the stress-strain relationship and pore pressure variation law of rock-soil mass materials. Li et al. [21] believed that the greater the unloading rate, the greater the damage degree to the expansive soil. Wang et al. [22] found that the axial strain, ultimate strength, and residual strength of the peak values of soft rocks were positively correlated with the unloading stress level and unloading rate.

Owing to the limitations of laboratory tests, field tests can simulate an actual project relatively well, and the test results are relatively reliable. Therefore, many scholars have studied the collapsibility of collapsible loess through field experiments.

Huang and Yang [23] summarized a large number of test pit immersion tests and found that the calculated value was lower than the actual value in the areas where the general calculated and measured collapsibility were quite different. In addition, the self-weight collapsibility was strong. Wang et al. [24] conducted an on-site immersion test in conjunction with the Xi'an subway project, studied the characteristics of loess collapsibility deformation at the site, and analyzed the changes in the collapsibility deformation speed with time. Huang et al. [25, 26] obtained the characteristics of a slow-fast-slow-stable collapse on the surface and in deep loess through an analysis of immersion in a field test pit. Liu [27] obtained the change characteristics of a cumulative settlement and collapse rate over time through an analysis of field test data.

In terms of these research statuses, the research on collapsible loess is divided into two parts. First, starting from the theoretical aspect, Zhujiang Shen and others established a binary medium model based on the structural properties of loess; Hu Zaiqiang, Fengji Zhu, Zhenghan Chen, Lingxia Gao, and others analyzed the influence of different factors on the characteristics of collapsible loess and established related theoretical research methods. Another part of scholars conducted indoor or on-site tests on collapsible loess under special conditions such as different levels of load conditions, different pH environments, and different moisture contents through a combination of theory and experimentation, through summarizing the laws and theoretical analysis, studying its characteristics.

It can be seen that many scholars have conducted research on loess collapsibility under constant pressure. However, they have failed to consider the impact of the upper pressure changes, and the relevant norms have mostly been derived from collapsibility theory under constant pressure. Thus, they cannot be accurately applied to underground space engineering under an unloading state and cannot meet the requirements of the engineering economy.

Jin et al. [28, 29] took the unloading collapsibility process of soil between piles in a loess site under water immersion as the background and started the initial research on the unloading collapsibility of loess. The test simulated the collapsibility process of immersion-pressurization-unloading and proposed an expression for the unloading loess collapse coefficient under these working conditions. However, in unloading projects such as subways and integrated pipe corridors, the mode of foundation treatment is usually unloading-immersion or unloading-immersion-pressurization.

Based on the above discussion, analysis, and summary, it remains necessary to study the collapse coefficient of loess under unloading. In this study, the characteristics and deformation mechanism of loess collapsibility under the unloading-immersion mode were studied through laboratory tests. An expression was established for the unloading collapse coefficient, and the accuracy of the calculation formula was verified using field monitoring test data. The research results of this study can provide a theoretical basis for an evaluation method for collapsibility in underground space engineering, provide help for research on the mechanical properties of collapsible loess and disaster prevention and mitigation in northwest China, and provide certain reference value for underground municipal engineering construction in loess areas.

2. Unloading Collapse Coefficient Expression

This article takes underground space engineering as the background and, based on the literature [29], quantitatively explores the variation law of the unloading collapse

coefficient under this working condition. The unloading collapse process is described based on the unloading stress ratio, unloading collapse ratio, and unloading collapse attenuation coefficient; based on this information, the unloading collapse coefficient and its coefficient expression are proposed.

2.1. Unloading Stress Ratio K. The unloading stress ratio K is defined to reflect the degree of the pressure reduction in the process of loess unloading:

$$K = \frac{P_0 - \Delta P}{P_0} = \frac{P_X}{P_0}, \tag{1}$$

where P_x is the upper pressure after unloading, in kPa; P_0 is the initial pressure, in kPa; ΔP is the unloading pressure, in kPa.

2.2. Unloading Collapse Ratio η. By defining the unloading collapse ratio η, the degree of the unloading collapsibility of the loess can be reflected:

$$\eta = \frac{S_1}{S} \times 100\%, \tag{2}$$

where S_1 is the unloading collapsibility of the loess, in mm, and S is the loess collapsibility under a constant pressure, in mm.

2.3. Unloading Collapsibility Attenuation Coefficient δ_r. Owing to the unloading effect, the collapsibility of the loess will be less than that with a constant pressure. To express the degree of collapsibility, the ratio of the relative collapse reduction S_r to the original height h_0 of the soil sample is defined as the unloading collapsibility attenuation coefficient δ_r:

$$\delta_r = \frac{S_r}{h_0}. \tag{3}$$

The unloading collapse process is shown in Figure 1. The BC section represents the total collapse amount S of the undisturbed soil under the initial pressure P_0, and the BD section represents the process of unloading the load ΔP from the initial pressure. The DE section represents the collapse amount S_1 of the sample under pressure P_x after being unloaded and immersed in water.

2.4. Unloading Collapse Coefficient δ_{xs}. The unloading collapse potential is expressed using the unloading collapse parameters of the loess, and the unloading collapse coefficient δ_{xs} is as follows:

$$\delta_{xs} = \delta_s - \delta_r, \tag{4}$$

where δ_s is the collapse coefficient under a constant pressure and can be calculated as follows:

$$\delta_s = \frac{S}{h_0}. \tag{5}$$

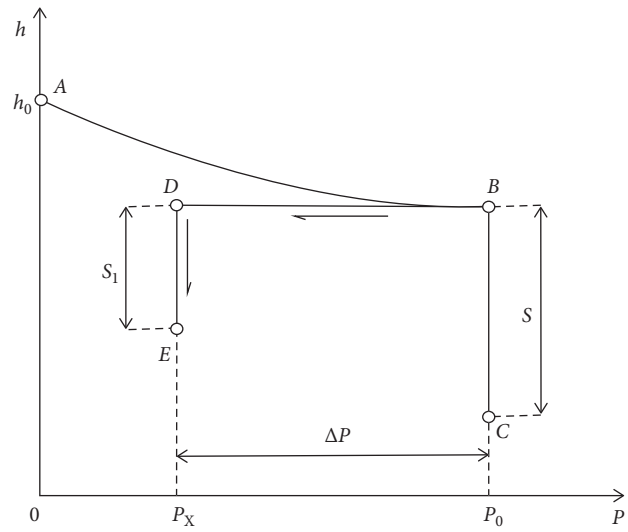

Figure 1: Unloading collapse process.

Substituting equations (2), (3), and (5) into (4), we obtain the expression as follows:

$$\delta_{xs} = \delta_s \eta. \tag{6}$$

It is not difficult to see that δ_{xs} is a reduction of δ_s and that η is equivalent to the reduction coefficient. For η, two parameters should be considered: the initial pressure P_0 and the unloading stress ratio K (reflecting the size of the unloading).

A functional relationship is used to represent η as follows:

$$\eta = f(K, P_0). \tag{7}$$

Therefore, an expression can be derived as follows:

$$\delta_{xs} = \delta_s f(K, P_0). \tag{8}$$

Equation (8) is the expression of the loess unloading collapse coefficient δ_{xs}.

To more intuitively understand the effect of unloading on the collapsibility of the loess, indoor collapsibility tests under constant pressure and unloaded loess were required. The change rule of the collapse coefficient of the collapsible loess under unloading was obtained by comparative analysis. The dominant factor in $f(K, P_0)$ was determined to be the unloading stress ratio K according to the laboratory test data. The functional relationship of η–K was analyzed, and a specific form for the expression of the outlet unloading collapse coefficient was finally fitted.

3. Laboratory Compression Test of Loess

The soil sample was taken from a construction site in the Tongchuan New District, Shaanxi Province. The terrain was flat, the geomorphic unit was single, and the collapsibility was strong. The basic physical indexes of the soil samples are shown in Table 1.

Table 1: Basic physical indexes of soil samples.

Buried depth (m)	Soil depth (m)	Natural moisture content (%)	The density of natural (g/cm^3)	Dry density (g/cm)	Severe (kN/cm^3)	Pore-solids ratio
5	5	10.800	1.487	1.321	14.7	1.134
10	10	13.700	1.516	1.307	15.0	1.065
15	15	18.610	1.649	1.334	15.9	0.955
20	20	18.890	1.750	1.419	17.4	0.836

3.1. Loess Collapsibility Test under Constant Pressure. In this study, the changes in the collapse coefficient and initial pressure of the loess under constant pressure at different buried depths were obtained through laboratory tests, and the collapsibility deformation characteristics of the loess were analyzed. The main test instruments comprised a W–G single rod consolidation apparatus, dial meter (0.01 mm), electrothermal-blast constant temperature drying box, and electronic balance. The test process was divided into two steps: soil sample preparation and loess collapsibility testing under constant pressure. The equipment picture and soil sample are shown in Figure 2.

When preparing the soil samples, a cutting ring with a height of 2 cm and area of 30 cm^2 was selected, and several undisturbed loess cutting ring samples were prepared, with depths of 5 m, 10 m, 15 m, and 20 m.

The loading pressure was determined according to the provisions of "Building Standards for Collapsible Loess Area" on the loading pressure of collapsible loess. When the buried depth is less than 10 m, take 200 kPa. When the depth is greater than 10 m, take the saturated self-weight pressure of the overlying soil. In combination with the "Standards for Geotechnical Test Methods" [30], a graded loading method was adopted. The pressure grade was set at 25 kPa and added to the specified pressure. The pressure grades are listed in Table 2.

3.2. Loess Subsidence Test under Unloading. The unloading collapsibility test was mainly divided into three steps: compression consolidation, unloading, and flooding. The specific scheme was as follows.

3.2.1. Test Sampling. Five pieces were placed at 5 m, 10 m, 15 m, and 20 m, respectively, for a total of 20 pieces, and then the pieces were weighted.

3.2.2. Consolidation Compression.

① Initial pressure setting: according to the "Building Standards in Collapsible Loess Area," the recommended initial pressure value of the soil layer within 10 m was 200 kPa, and the saturated dead weight pressure of the overburden soil under 10 m was taken. According to the geological exploration report calculation, the saturated dead weight pressure P_z and initial pressure P_0 values of the overburden soil as borne by the soil at 5 m, 10 m, 15 m, and 20 m are shown in Table 3.

② The pressure: the sample was compressed and consolidated with the W–G single rod type consolidation instrument. The initial pressure was increased step by step to P_0, and the data were recorded after the deformation stabilized.

3.2.3. Unloading Treatment. Based on referring to the pressure grade, the unloading quantity $\triangle P$ was classified into 25 kPa, 50 kPa, 75 kPa, and 100 kPa. The upper pressure after unloading is shown in Table 4.

3.2.4. Immersion. After unloading, the upper pressure was kept unchanged, the sample was immersed in water, and the deformation reading of the sample was observed as stable.

3.3. Analysis of Test Results. The trend of the loess (δ_{xs}–P_x) under unloading was obtained through laboratory tests, as shown in Figure 3.

It can be seen from Figure 3 that the relationship between the loess collapse coefficient and upper pressure after unloading is as follows:

① The change relationship of the loess (δ_{xs}–P_x) under unloading conforms to the trend of constant pressure collapsibility; that is, it occurs in two stages, the compaction stage and unloading collapsibility stage. In the compaction stage, the structural properties of the loess are not completely destroyed but still have a certain strength, and the structure is relatively compact. In the unloading collapse stage, the upper pressure increases to near the initial pressure of the collapse, and the soil produces collapse and deformation. This develops rapidly until the deformation stabilizes.

② The collapsibility of the loess under unloading is related to the buried depth of the soil. The greater the buried depth, the tighter the connection of the soil particles, the smaller the porosity, and the weaker the collapsibility; the greater the buried depth, the greater the initial pressure of the collapsibility, and the more delayed the process of collapse.

A comparison of the constant pressure, unloading collapse coefficient, and pressure curve is shown in Figure 4.

From a comparative analysis of the constant pressure and unloading collapse coefficient and pressure curve in Figure 4, the following conclusions can be drawn:

① The unloading and constant pressure collapse coefficient of the loess has the same general trend as the pressure curve, showing an increasing curve, but the

(a) (b)

Figure 2: Test instrument and samples.

Table 2: Loading pressure gauge.

Buried depth (m)	Pressure settings (kPa)							
5	25	50	75	100	125	150	175	200
10	25	50	75	100	125	150	175	200
15	100	200	225	250	275	300		
20	100	200	300	325	350	375	400	

Table 3: Setting table of saturated dead weight pressure and initial pressure of overburden soil.

Buried depth (m)	5	10	15	20
P_z (kPa)	89.11	180.515	274.25	370.82
P_0 (kPa)	200	200	300	400

Table 4: Test scheme of loess collapsibility under unloading.

Buried depth (m)	Initial pressure P_0 (kPa)	Unloading quantity (kPa)	Upper pressure after unloading P_x (kPa)
5	200	25/50/75/100	175/150/125/100
10	200	25/50/75/100	175/150/125/100
15	300	25/50/75/100	275/250/225/200
20	400	25/50/75/100	375/350/325/300

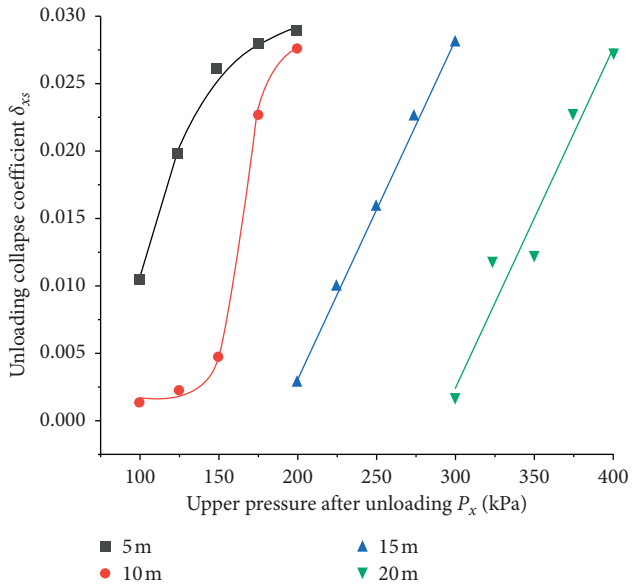

Figure 3: Loess curve of δ_{xs}–P_x.

unloading collapse coefficient is always smaller than the constant pressure collapse coefficient. Under the action of the initial pressure, the soil is compacted and consolidated, and the porosity is reduced. After unloading, as the upper pressure cannot reach the original compaction and stability corresponding to the structural failure conditions, the soil continues to deform after immersion, but the additional deformation is reduced relative to that at the constant pressure condition. Under the corresponding unloading action, the collapse coefficient decreases, but the trends of the two curves are close, and the corresponding pressures at the characteristic points of the curves are similar.

② The collapse coefficient for unloading the loess at a low pressure is small, and the difference from the constant pressure increases with increases in pressure; moreover, the two curves are more separated. However, when the pressure increases to a certain limit value, the coefficient difference reaches a peak value. After that, the slope of the unloading curve increases sharply, the unloading collapse rate is greater than the constant pressure collapse rate, and the two curves gradually become close. The unloading curve slope inflection point is taken as the unloading collapse limit point, and the corresponding pressure is the limit pressure. It can be seen from Figure 4 that the limit pressure is always less than the initial pressure of the collapse. Therefore, it can be said that the unloading effect increases the initial pressure of the collapsibility of the loess to a certain extent.

Compared with constant pressure subsidence, unloading can increase the initial subsidence pressure of the loess, and the greater the burial depth, the more evident the improvement. As can be seen from Figure 3, the initial subsidence pressure of the soil at 5 m increased from 109.4 kPa under constant pressure to 111.3 kPa, an increase of 1.5%. The initial subsidence pressure of the soil at 10 m increased from 169.2 kPa under constant pressure to 172.3 kPa, an increase of 1.8%. The initial subsidence pressure of the soil at 15 m increased from 216.8 kPa under constant pressure to 235.5 kPa, an increase of 8.6%. The initial subsidence pressure of the soil at 20 m increased from 331.6 kPa under constant pressure to 362.5 kPa, an increase of 9.3%.

3.4. Determination of the Expression for the Unloading Collapse Coefficient. An orthogonal test was conducted based on the results of the unloading collapsible test. First, the two affecting factors were determined: K and P_0. Second, the level of each factor was determined: K was taken as 0.8, 0.6, and 0.4, and the P_0 pairs had three test levels: 200, 300, and 400.

In Table 5, L_n is the sum of the results of the respective levels of the factors, Ln' is the mean value of the sum of the results of the respective levels of the factors, and R is the range of the factors.

The results are shown in Table 5. According to the R range analysis of the results, the range for K (0.41) is much larger than the range for P_0 (0.04), indicating that, within a reasonable range of change, K has a much greater influence on the target result than P_0. In other words, the unloading stress ratio K has the greatest influence on the η function; K is an important factor, and the initial pressure P_0 is a secondary factor. In summary, the unloading stress ratio K plays a major role in controlling the collapsible deformation of the loess under unloading.

K is also taken as an important factor in the fitting expression $f(K, P_0)$, according to the orthogonal test results. The K–η function is used to fit the unloading test for the soil at 10 m, as shown in Figure 5. It can be seen that the fitting function is approximately an exponential function, so it is expressed by the expression of the exponential function as follows:

$$f(K) = ae^{-(1/b)x} + c, \tag{9}$$

where a, b, and c are all parameters. A further regression analysis was conducted on all of the unloading collapsibility test data from the laboratory test to determine the fitting curve parameters, as shown in Table 6.

The mean values of parameters a, b, and c in Table 6 are substituted into $f(K)$ to determine the expression for the unloading collapse coefficient as follows:

$$\delta_{xs} = \delta_s f(K) = 0.09e^{(1/0.4)K}\delta_s. \tag{10}$$

To verify the correctness of the unloading collapse coefficient, the results calculated using equation (10) are compared with the test results; the comparison curve is shown in Figure 5. It can be seen that the unloading collapse coefficient expression can better fit the collapse coefficient under different dead weight pressures.

In Figure 6, the calculated value obtained by the expression of the unloading collapse coefficient is basically consistent with the trend of the experimental value curve. The experimental value is generally slightly larger than the calculated value, but the difference does not exceed 0.005. In addition, if the collapse coefficient remains as 0.015, that is, as the limit for judging collapsibility, it can be found that the difference between the calculated initial pressure of the collapsibility and test value will not exceed 5%.

4. Field Test

According to the survey report and "Building Standards for Collapsible Loess Areas," resampling was conducted at the site, and the original loess samples at 1 m – 10 m below the ground (layered height of 1 m) were collected using boreholes. Indoor tests were conducted to obtain the collapse coefficient. The unloading collapse coefficient and total collapsibility were calculated as shown in Tables 7 and 8, and then the self-weight collapse coefficient and self-weight collapsibility were calculated as shown in Tables 9 and 10. The saturation pressure was calculated from the specific

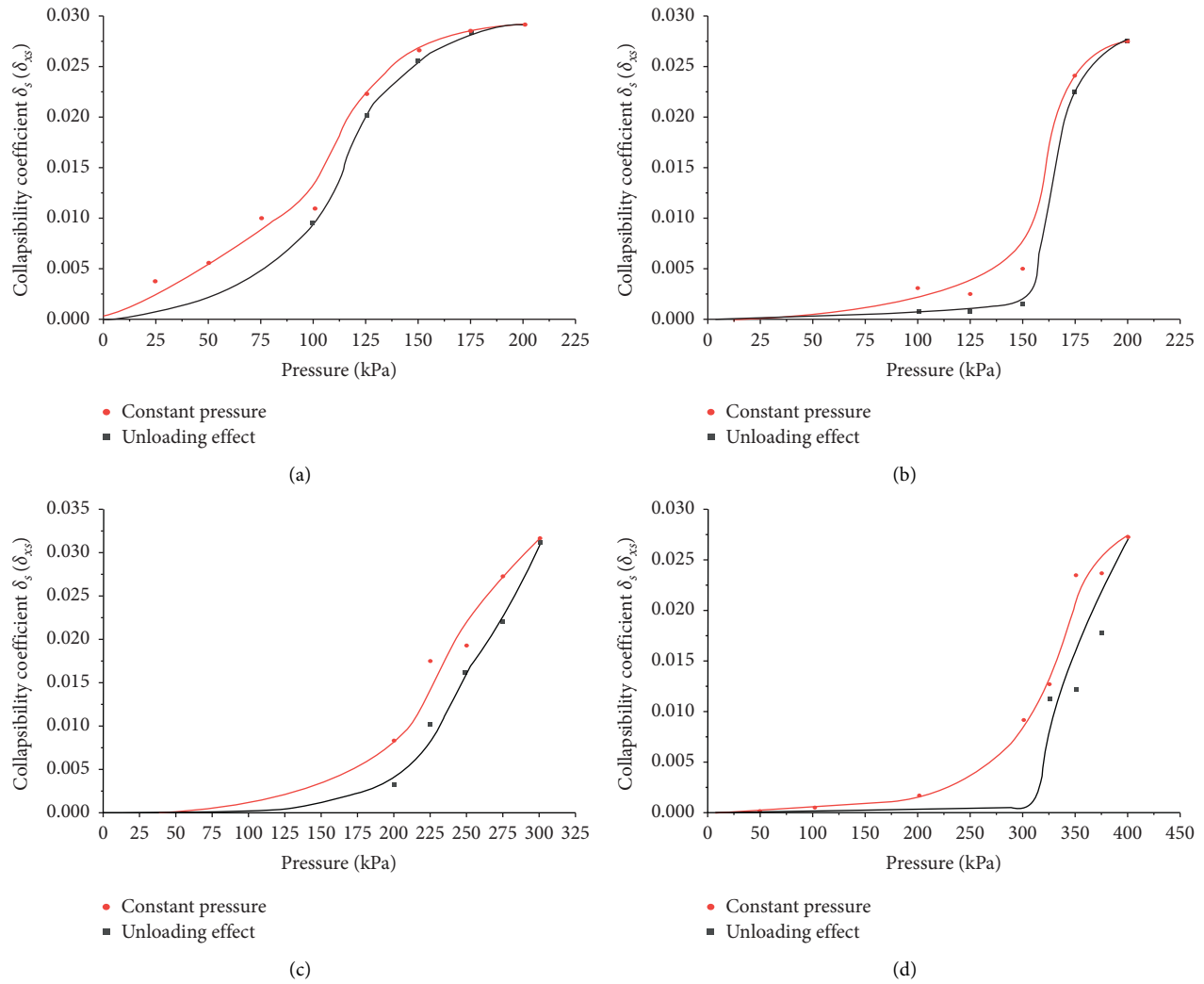

Figure 4: Comparison of constant pressure and unloading collapse coefficient and pressure curve. (a) 5 m. (b) 10 m. (c) 15 m. (d) 20 m.

Table 5: Orthogonal test results.

Serial number	Factors		η
	K	P_0	
1	0.8	200	0.58
2	0.8	300	0.55
3	0.8	400	0.52
4	0.6	200	0.32
5	0.6	300	0.29
6	0.6	400	0.28
7	0.4	200	0.16
8	0.4	300	0.13
9	0.4	400	0.12
L1	1.65	1.06	
L2	0.89	0.97	
L3	0.41	0.92	
L1′	0.55	0.35	
L2′	0.30	0.32	
L3′	0.14	0.31	
R	0.41	0.04	

gravity and pore-solids ratio of the soil; the removal of 2 m of soil was equivalent to unloading at 28 kPa, and its saturation pressure was 35 kPa.

In Tables 7–10, the self-weight collapsibility calculated from the unloading collapse coefficient is 120 mm, and the total collapsibility is 468.5 mm. The self-weight collapse coefficient as calculated by the constant pressure test is 314.4 mm, and the total subsidence is 609.5 mm. To further verify the applicability of the expression for the unloading collapse coefficient, a comparative analysis was conducted through field industrial tests.

4.1. Test Scheme. To simulate the unloading conditions of underground space engineering, the foundation pit was excavated at a depth of 2 m. It was determined that the soil layer in the flooded pit was in the unloading state under a saturated deadweight stress. The surface of the foundation pit was taken as the design surface.

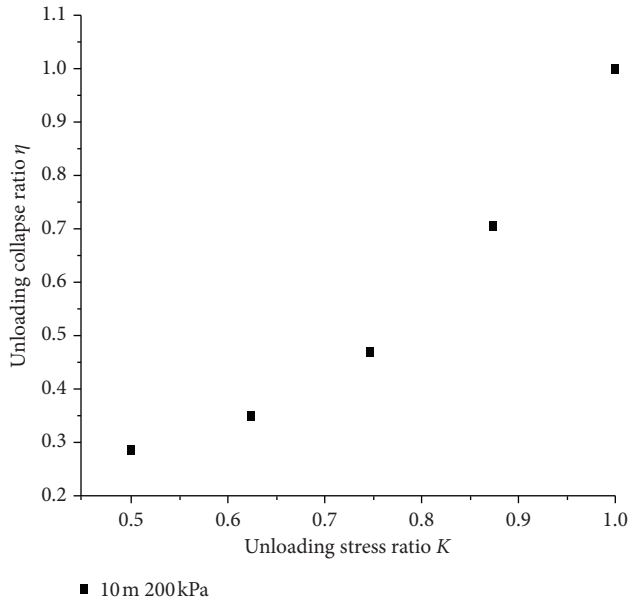

Figure 5: Fitting curve (10 m 200 kPa).

Table 6: η–K fitting parameters.

Buried depth (m)	P_0 (kPa)	a	b	c	R
10	200	0.090	−0.4	−0.07	0.99
15	300	0.099	−0.42	−0.08	0.98
20	400	0.081	−0.38	−0.05	0.99

The area of the immersion test pit was 8100 mm × 7200 mm. To measure the amount of collapsibility and deformation of the formation, 12 stratum subsidence observation punctuation points were set up in the pit, and holes with a diameter of 120 mm were drilled at the punctuation points. The punctuation points were taken at six measuring depths, namely, 1 m, 2 m, 3 m, 5 m, 8 m, and 10 m; each depth was composed of two measuring points as a group, for a total of six groups. A benchmark was made, and a measuring ruler was placed on its surface. The reference point for the observation data was set up on the periphery of the test pit and 1 m away from the edge of the test pit.

To ensure that the soil layer of the site was fully soaked, 32 water injection holes with a diameter of 400 mm and depth of 12 m were arranged in the test pit, and all water injection holes were evenly distributed. The test pit diagram is shown in Figure 7.

The duration of immersion was 7 days, and the immersions began at the same time and continued for 26 days. In the process of water immersion, the level was used to observe the benchmark every day, and the settlement amounts of the stratum at 1 m, 2 m, 3 m, 5 m, 8 m, and 10 m in the pit were observed, respectively. The observation accuracy was controlled to be within the specified range. The layout of monitoring points is shown in Figure 8.

4.2. Analysis of Test Results. This test lasted for 26 days, and the entire process was monitored, that is, from the immersion of the test pit to the settlement and deformation stability of the foundation. The variation in the formation settlement over time is shown in Figure 9.

It can be seen from Figure 9 that the formation settlement rate is divided into three stages. In the first stage (0 – 5 days), the water has just begun to infiltrate, the soil is not fully soaked, and the settlement deformation is small, accounting for approximately 5% – 15% of the total settlement. In the second stage (6 – 15 days), the settlement rate of each soil layer in this stage increases sharply, corresponding to the steep drop section in the curve of Figure 9. The settlement amount accounts for approximately 64% – 75% of the total settlement amount. In the third stage (16 – 26 days), the settlement amount is small, the settlement rate gradually tends to be stable, and the settlement process is basically complete. The settlement amount in this stage accounts for approximately 10%–31% of the total settlement amount.

The final observed settlement amount for each soil layer is shown in Table 11. The final settlement of the soil at 10 m is 9.8 mm, and that of soil at 1 m is 83.4 mm. That is, the deeper the soil is buried, the smaller the unloaded subsidence is, and the weaker the collapsibility of the soil is. Therefore, it can be inferred that the surface settlement is approximately 85–95 mm, which can be used as the field settlement test value.

In summary, in Table 10, the amount of collapsibility as calculated by the unloading collapse coefficient is 120 mm, and the amount of subsidence as obtained by the constant pressure test coefficient is 314.4 mm. Therefore, compared with the surface subsidence value obtained by the field tests (85–95 mm), the amount of subsidence calculated by the unloading coefficient is evidently closer to it. The wet fall at the same time from using the specification of the constant pressure coefficient should be used to calculate the collapsibility of the total quantity and amount for the collapsibility level, that is, to determine the collapse grade, and

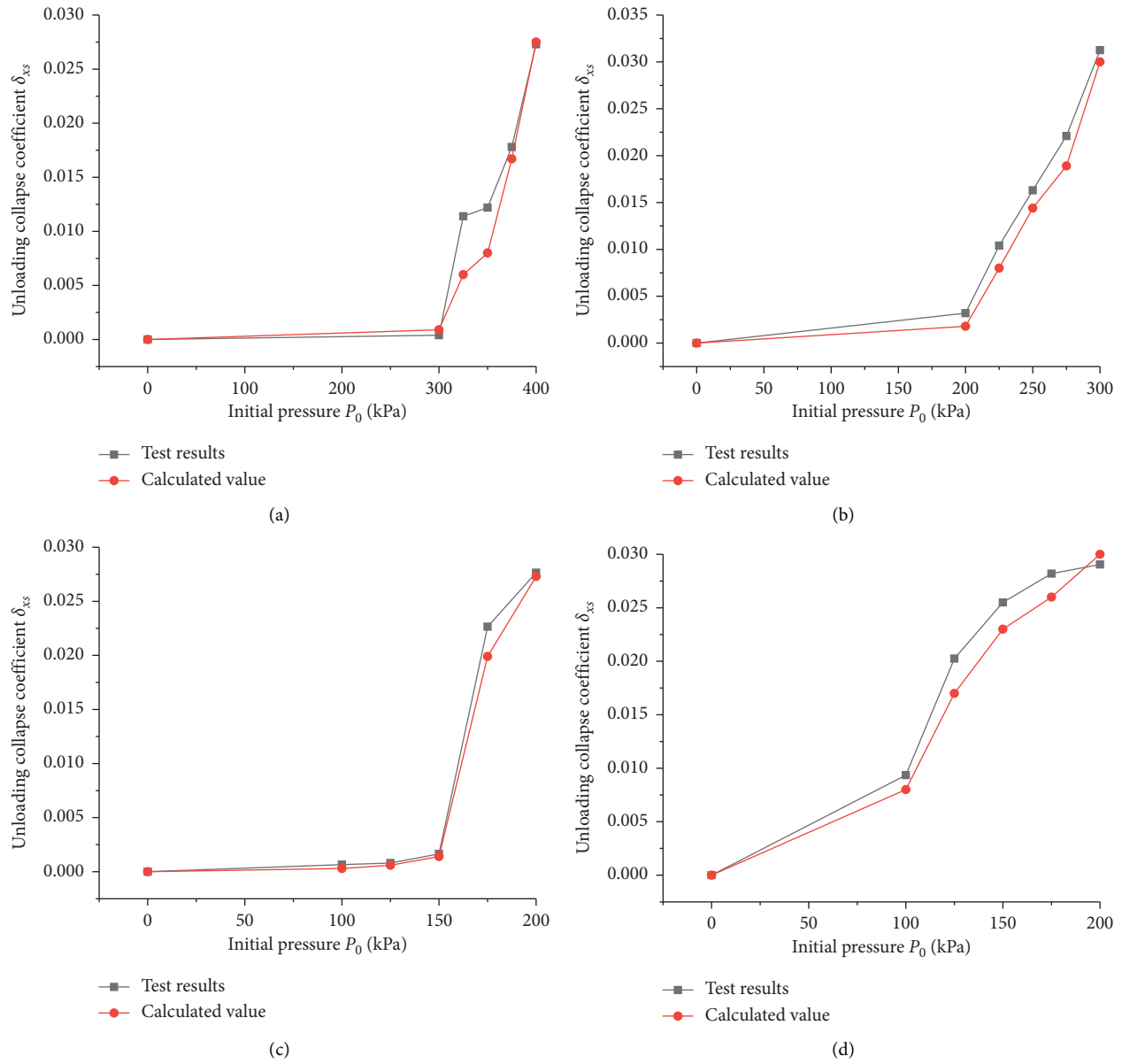

Figure 6: Comparison between the experimental value of δ_{xs} and the calculated value. (a) 20 m, 400 kPa. (b) 15 m, 300 kPa. (c) 10 m, 200 kPa. (d) 5 m, 100 kPa.

Table 7: Coefficient of constant pressure and unloading coefficient of subsidence.

Buried depth (m)	Initial pressure (kPa)	Unloading quantity (kPa)	Upper pressure after unloading (kPa)	Unloading stress ratio K	δ_S	Unloading collapse coefficient δ_{xs}
1	200	28	172	0.86	0.073	0.056
2	200	28	172	0.86	0.061	0.047
3	200	28	172	0.86	0.069	0.053
4	200	28	172	0.86	0.056	0.043
5	200	28	172	0.86	0.05	0.039
6	200	28	172	0.86	0.043	0.033
7	200	28	172	0.86	0.039	0.030
8	200	28	172	0.86	0.035	0.027
9	200	28	172	0.86	0.033	0.025
10	200	28	172	0.86	0.021	0.016

Table 8: Calculation table of total collapsibility.

Buried depth (m)	Unloading collapse coefficient	Constant pressure coefficient of wetting	Thickness (mm)	Correction coefficient	The total amount of wetting (mm)	
					Unloading	Constant
1	0.056	0.073	1000	1.5	84.0	109.5
2	0.047	0.061	1000	1.5	70.5	91.5
3	0.053	0.069	1000	1.5	79.5	103.5
4	0.043	0.056	1000	1.5	64.5	84
5	0.039	0.05	1000	1	39.0	50
6	0.033	0.043	1000	1	33.0	43
7	0.030	0.039	1000	1	30.0	39
8	0.027	0.035	1000	1	27.0	35
9	0.025	0.033	1000	1	25.0	33
10	0.016	0.021	1000	1	16.0	21
Sum					468.5	609.5

Table 9: Self-weight collapse coefficient.

Saturation deadweight pressure (kPa)	Unloading quantity (kPa)	Upper pressure after unloading (kPa)	Unloading stress ratio K	δ_{zS}	Unloading self-weight collapse coefficient δ_{xzs}
51	35	16	0.31	0.024	0.005
74	35	39	0.53	0.020	0.007
87	35	52	0.60	0.030	0.012
104	35	69	0.66	0.025	0.012
119	35	84	0.71	0.032	0.017
137	35	102	0.74	0.030	0.017
151	35	116	0.77	0.026	0.016
176	35	141	0.80	0.023	0.015
195	35	160	0.82	0.029	0.020
209	35	174	0.83	0.021	0.015

Table 10: Calculation table of self-weight collapsibility.

Buried depth (m)	δ_{xzs}	δ_{zS}	Thickness (mm)	Correction coefficient	The calculated value of the collapsibility (mm)	
					Unloading	Constant
1	0.005	0.024	1000	1.2	0.0	28.8
2	0.007	0.020	1000	1.2	0.0	24.0
3	0.012	0.032	1000	1.2	0.0	38.4
4	0.012	0.025	1000	1.2	0.0	30.0
5	0.017	0.032	1000	1.2	20.4	38.4
6	0.017	0.030	1000	1.2	20.4	36.0
7	0.016	0.026	1000	1.2	19.2	31.2
8	0.015	0.023	1000	1.2	18	27.6
9	0.020	0.029	1000	1.2	24	34.8
10	0.015	0.021	1000	1.2	18	25.2
Sum					120	314.4

Figure 7: Site test pit map.

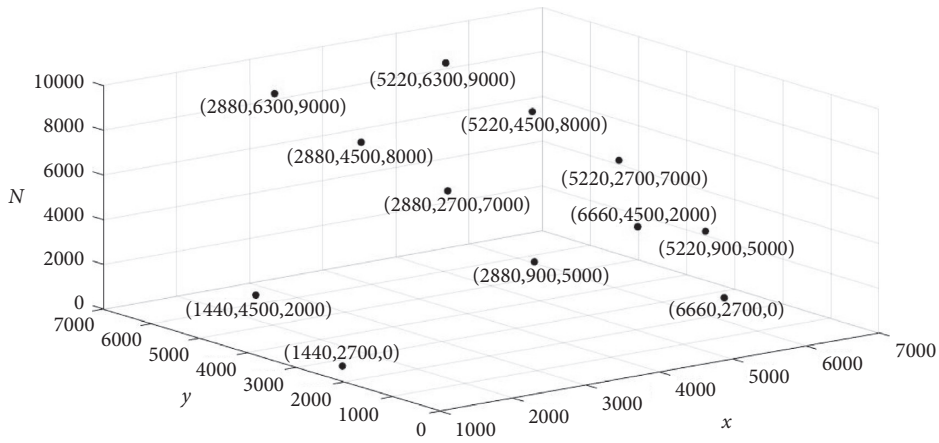

Figure 8: Layout plan of monitoring points.

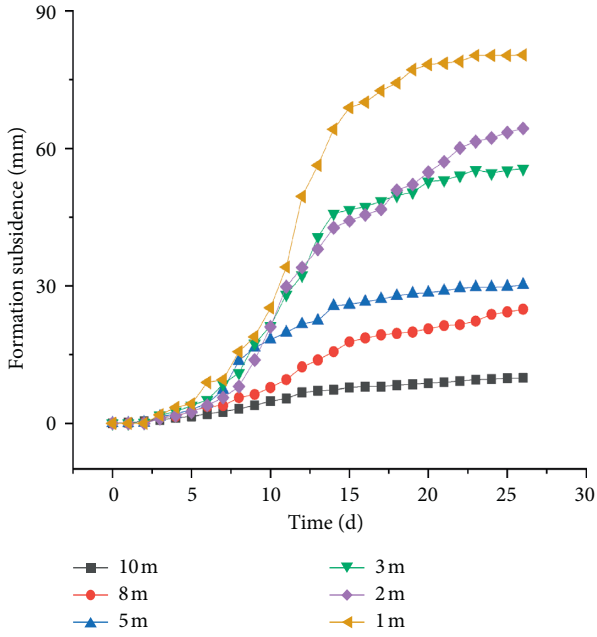

Figure 9: Variation of formation settlement over time.

should be judged as level III (serious). That from using the wet unloading test of the ground should be judged as level II (medium). The main reason is that there will be a layer of soil subsidence under a constant pressure, but there is no subsidence after unloading. Therefore, one less layer of soil will be considered when calculating the subsidence amount, resulting in a large difference in the result.

Therefore, it can be seen that the criterion has certain limitations in the collapsibility evaluation of loess. When unloading of the loess foundation occurs, the collapsibility evaluation is too conservative, greatly increasing the project budget. However, the total and self-weight collapsibility as calculated by the unloading coefficient are more in line with reality, indicating the necessity and feasibility of this research content.

Table 11: Formation settlement amount.

Buried depth (m)	1	2	3	5	8	10
Settlement (mm)	83.4	62.4	55.3	29.8	22.4	9.8

5. Conclusions

In this study, collapsible loess under unloading was examined. An unloading collapse coefficient expression was established and then analyzed and verified using field tests.

(1) Based on the unloading stress ratio K, unloading collapsible ratio η, and attenuation coefficient δ_r of the unloading collapsibility, an expression is established for the unloading collapse coefficient, and the functional form and specific parameters of the expression are determined from laboratory tests.

(2) Through the laboratory tests, it is found that unloading can increase the initial pressure of the collapsibility to a certain extent, with an increase of 1.5 – 9.3%. Moreover, the deeper the soil is buried, the greater the increase is.

(3) The total and deadweight collapsibility as calculated using the unloading coefficient of the collapsibility can more accurately and reliably evaluate the collapsibility of a site under the action of unloading.

Regarding unloading project, the existing codes cannot make an accurate collapsibility evaluation for it. The total collapsibility and self-weight collapsibility calculated by the constant pressure collapsibility coefficient in the specification are used to determine the site's collapsibility level as III (severe), and the site's collapsibility level should be determined as level II (medium) when using the collapsibility under the unloading test. It can be seen that the unloading collapsibility coefficient is more suitable for unloading projects than the constant pressure collapsibility coefficient.

Data Availability

No data were used to support this study.

Conflicts of Interest

The authors declare that there are no conflicts of interest regarding the publication of this paper.

Acknowledgments

This work was supported by General Project of Science and Technology of Shaanxi Province, named as Research on Key Technologies of Evaluation and Treatment of Collapsible Loess Foundation of Urban Underground Municipal Engineering (2020SF–431).

References

[1] GB-50025-2018, "Code for building construction in collapsible loess regions," 2018, http://codeofchina.com/standard/GB50025-2004.html.

[2] Z. D. Liu and B. P. Zhang, "Concerning the evaluation of hydroeonsolidation characterization of loess and loess soil," *Chinese Journal of Geotechnical Engineering*, vol. 2, no. 4, pp. 22–33, 1980.

[3] Y. S. Luo, "Assessment of collapsibility of collapsible loess foundation," *Chinese Journal of Geotechnical Engineering*, vol. 20, no. 4, pp. 90–94, 1998.

[4] Z. H. Chen and Z. D. Liu, "Mechanism of collapsible deformation of loess," *Chinese Journal of Geotechnical Engineering*, vol. 8, no. 2, pp. 3–14, 1986.

[5] S. J. Shao, C. M. Yang, X. T. Ma, and S. Lu, "Correlation analysis of collapsible parameters and independent physical indices of loess," *Rock and Soil Mechanics*, vol. 34, no. 2, pp. 27–34, 2013.

[6] A. M. Assallay, C. D. F. Rogers, and I. J. Smalley, "Formation and collapse of metastable particle packings and open structures in loess deposits," *Engineering Geology*, vol. 48, no. 1-2, pp. 101–115, 1997.

[7] A. M. Assallay, I. Jefferson, C. D. F. Rogers, and I. J. Smalley, "Fragipan formation in loess soils: development of the Bryant hydroconsolidation hypothesis," *Geoderma*, vol. 83, no. 1, pp. 1–16, 1998.

[8] Z. J. Shen and Z. Q. Hu, "Binary medium model for loess," *Journal of Hydraulic Engineering*, vol. 7, pp. 3–8, 2003.

[9] S. J. Shao, C. M. Yang, X. T. Ma, and S. Lu, "Correlation analysis of collapsible parameters and independent physical indices of loess," *Rock and Soil Mechanics*, vol. 36, no. 2, pp. 1–6, 2005.

[10] F. J. Zhu, J. J. Nan, Y. Q. Wei, and L. Bai, "Mathematical statistical analysis on factors affecting collapsible of loess," *The Chinese Journal of Geological Hazard and Control*, vol. 30, no. 2, pp. 128–133, 2019.

[11] Z. D. Liu, "Analysis of factors affecting loess collapsibility coefficient," *Geotechnical Investigation & Surveying*, no. 5, pp. 6–11, 1994.

[12] S. F. Wang and D. L. Liu, "Correction of collapsibility index of loess," *Site Investigation Science and Technology*, no. 5, pp. 29–31, 2002.

[13] Z. Q. Hu, Y. Zhang, W. Q. Yue et al., "Collapsible tests of loess under acid conditions and related sensitivity analysis," *Chinese Journal of Rock Mechanics and Engineering*, vol. 36, no. 7, pp. 1748–1756, 2017.

[14] Y. Zhang, *Study on evolution of loess structure and its constitutive model in acidic environment*, Ph.D. thesis, Xi'an University of Technology, Xi'an, China, 2019.

[15] Z. H. Chen and N. Guo, "New developments of mechanics and application for unsaturated soils and special soils," *Rock and Soil Mechanics*, vol. 40, no. 1, pp. 1–54, 2019.

[16] Y. L. Zhou, X. P. Wu, and J. H. Fang, "Comparative study on field and laboratory tests for collapsibility characteristics of large thickness loess," *Railway Engineering*, vol. 58, no. 1, pp. 1–54, 2018.

[17] S. J. Shao, J. Li, G. L. Li et al., "Evaluation method for self-weight collapsible deformation of large thickness loess foundation," *Chinese Journal of Geotechnical Engineering*, vol. 37, no. 6, pp. 965–978, 2015.

[18] L. X. Gao, M. T. Luan, and Q. Yang, "Evaluation of loess collapsibility based on principal components of microstructural parameters," *Rock and Soil Mechanics*, vol. 33, no. 7, pp. 1921–1926, 2012.

[19] A. W. Yang, S. K. Yang, and Z. D. Zhang, "Experimental study of mechanical properties of dredger fill under different unloading rates and stress paths," *Rock and Soil Mechanics*, vol. 41, no. 9, pp. 2891–2900, 2020.

[20] W. S. Xu, G. M. Zhao, and X. R. Meng, "Effects of unloading rate on energy evolution mechanism in the single-side unloading failure of highly stressed marble," *Advances in Civil Engineering*, vol. 2020, Article ID 4185624, 11 pages, 2020.

[21] X. M. Li, L. W. Kong, and A. G. Guo, "Experimental study on shear mechanical properties of unloading damaged undisturbed expansive soil," *Rock and Soil Mechanics*, vol. 40, no. 12, pp. 4685–4692, 2019.

[22] L. H. Wang, C. Y. Niu, B. Y. Zhang et al., "Experimental study on mechanical properties of deep-buried soft rock under different stress paths," *Chinese Journal of Rock Mechanics and Engineering*, vol. 38, no. 5, 2019.

[23] X. F. Huang and X. H. Yang, "A study progress on in-situ soaking test on collapsible loess," *Rock and Soil Mechanics*, vol. 34, no. 2, pp. 222–228, 2013.

[24] Q. M. Wang, K. C. Li, H. W. Gu, and Z. Kang, "Application of field test pit immersion test in Subway Engineering in collapsible Loess Regions," *Ground Water*, vol. 41, no. 1, pp. 115–120, 2019.

[25] X. E. Huang, Z. H. Chen, S. Ha et al., "Large area field immersion tests on characteristics of deformation of self weight collapse loess under overburden pressure," *Chinese Journal of Geotechnical Engineering*, vol. 28, no. 3, pp. 107–114, 2006.

[26] X. P. Wu, *Study on the characteristics of collapse and permeability of large thickness loess ground based on water immersion test*, PhD thesis, Lanzhou University, Lanzhou, Gansu, China, 2016.

[27] N. Liu, *Study on the experimental of collapsible loess with dead weight in Guanzhong area*, Ph.D. thesis, Changan University, Xi'an, China, 2013.

[28] X. Jin, T. H. Wang, Z. K. Zhao, and Y. Luo, "Method for calculating coefficient of collapsibility of loess under unloading," *Chinese Journal of Geotechnical Engineering*, vol. 41, no. 10, pp. 1959–1966, 2019.

[29] T. H. Wang, X. Jin, Y. Luo, and S. L. Zhang, "A method for evaluation of loess collapse potential of unloading," *Rock and Soil Mechanics*, vol. 40, no. 4, pp. 1281–1290, 2019.

[30] GB/T 50123-2019, "Standard geotechnical test methods," 2019, https://codeofchina.com/standard/GBT50123-2019.html.